Predictions of HMA Permeability Using 3-D Microstructure Simulation of Fluid Flow

E. Masad[1], A. Al-Omari[2]

Summary

A numerical scheme is used in this study to simulate fluid flow in three dimensional (3-D) microstructures. The governing equations for the steady incompressible flow are solved using the Semi-Implicit Method for Pressure-Linked Equations (SIMPLE) finite difference scheme within a non-staggered grid system that represents the 3-D microstructure. An X-ray Computed Tomography (CT) system is used to capture the 3-D microstructures. The HMA specimens included field cores, laboratory linear kneading compactor (LKC) specimens, and laboratory Superpave gyratory compactor (SGC) specimens. The numerical permeability results are compared with closed form solutions.

Introduction

Permeability of asphalt mixes, as in other porous media, is a function of air void distribution characteristics such as number, size, and percent of air voids (%AV). The difficulty of quantifying this distribution in porous media has led to a number of studies directed at the calculation of permeability by solving the fluid flow equations numerically within the boundary conditions of artificial or real microstructures of porous media. Adler *et al.* [1] and Martys *et al.* [2] generated isotropic artificial media and solved the Stokes equations in that media assuming Newtonian fluids with low Reynolds number (Re) fluid flow. Masad *et al.* [3] and Tashman *et al.* [4] solved Navier-Stokes equations in 2-D anisotropic microstructure of soil specimens. These numerical models account for the effect of the microstructure of the porous media directly and without the need to characterize the complex microstructure of the analyzed porous media.

In these numerical models, either a staggered or non-staggered scheme is used to solve the governing equations of the fluid flow. Adler *et al.* [1], Martys *et al.* [2], and Masad *et al.* [3] used the staggered scheme in which there are two different cells to be dealt with; one is the continuity cell and the other is the momentum cell. The non-staggered scheme was used by Tashman *et al.* [4] in simulating the fluid flow in two-dimensional (2-D) granular microstructures where only one cell is needed to solve for the continuity and Navier-Stokes equations. Al-Omari and Masad [5] developed a non-staggered finite difference numerical model for the simulation of steady incompressible fluid flow in three-dimensional (3-D) microstructures. They studied the numerical factors

[1] Assistant Professor, Department of Civil Engineering, Texas A&M University, College Station, TX 77843-3135
[2] Graduate Research Assistant, Department of Civil Engineering, Texas A&M University, College Station, TX 77843-3135.

such as convergence criterion and image resolution that might affect the simulation of fluid flow in 3-D microstructures. They also presented verifications of the developed numerical solution through comparisons with closed form solutions of idealized geometries such as packing of spheres and parallel fissures. In this study, the numerical simulation developed by Al-Omari and Masad [5] is used to calculate the HMA permeability and the numerical predictions are then compared to closed form solutions.

Simulation of Fluid Flow and Permeability

A finite difference program is developed to simulate the incompressible fluid flow in 3-D porous microstructures. The velocity fields within the microstructure is assumed to be driven only by pressure difference ($\Delta P=P_{inlet}-P_{outlet}$) between the inlet ($P_{inlet}$) and outlet ($P_{outlet}$) of this microstructure. The governing equations for the 3-D steady incompressible fluid flow are:

$$\frac{\partial \rho u}{\partial x}+\frac{\partial \rho v}{\partial y}+\frac{\partial \rho w}{\partial z}=0 \tag{1}$$

$$\frac{\partial}{\partial x}\left(\rho uu-\mu\frac{\partial u}{\partial x}\right)+\frac{\partial}{\partial y}\left(\rho uv-\mu\frac{\partial u}{\partial y}\right)+\frac{\partial}{\partial z}\left(\rho uw-\mu\frac{\partial u}{\partial z}\right)=-\frac{\partial P}{\partial x}+\frac{\partial}{\partial x}\left(\mu\frac{\partial u}{\partial x}\right)+\frac{\partial}{\partial y}\left(\mu\frac{\partial v}{\partial x}\right)+\frac{\partial}{\partial z}\left(\mu\frac{\partial w}{\partial x}\right) \tag{2}$$

$$\frac{\partial}{\partial y}\left(\rho vv-\mu\frac{\partial v}{\partial y}\right)+\frac{\partial}{\partial x}\left(\rho vu-\mu\frac{\partial v}{\partial x}\right)+\frac{\partial}{\partial z}\left(\rho vw-\mu\frac{\partial v}{\partial z}\right)=-\frac{\partial P}{\partial y}+\frac{\partial}{\partial y}\left(\mu\frac{\partial v}{\partial y}\right)+\frac{\partial}{\partial x}\left(\mu\frac{\partial u}{\partial y}\right)+\frac{\partial}{\partial z}\left(\mu\frac{\partial w}{\partial y}\right) \tag{3}$$

$$\frac{\partial}{\partial z}\left(\rho ww-\mu\frac{\partial w}{\partial z}\right)+\frac{\partial}{\partial x}\left(\rho wu-\mu\frac{\partial w}{\partial x}\right)+\frac{\partial}{\partial y}\left(\rho wv-\mu\frac{\partial w}{\partial z}\right)=-\frac{\partial P}{\partial z}+\frac{\partial}{\partial z}\left(\mu\frac{\partial w}{\partial z}\right)+\frac{\partial}{\partial x}\left(\mu\frac{\partial u}{\partial z}\right)+\frac{\partial}{\partial y}\left(\mu\frac{\partial v}{\partial z}\right) \tag{4}$$

In the above equations, u, v, and w are velocity components in the x-, y-, and z-directions, respectively. P represents the applied pressure, ρ and μ are fluid density and viscosity, respectively.

The finite difference model is based on the non-staggered numerical scheme that uses only one cell to solve the governing equations. Al-Omari and Masad [5] includes the details on the development of the numerical solution of these equations.

Darcy's law can be used in determining the fluid absolute permeability tensor (K) as follows:

$$\vec{V}=-\frac{1}{\mu}\mathrm{K}\cdot\nabla\overset{\rho}{P} \tag{5}$$

In Equation (5), $\vec{V}$ is the average velocity vector within the analyzed microstructure. K is the absolute permeability tensor. $\nabla\overset{\rho}{P}$ is the pressure gradient which is applied as the only driving force of the velocity fields within the microstructure. μ is the viscosity

coefficient of the fluid. The absolute permeability tensor, K, has the units of (m^2). Equation (6) is used to calculate the Darcy's permeability with units of (m/s):

$$k = K\frac{\gamma}{\mu} \tag{6}$$

where γ is the unit weight of the fluid, and μ is the fluid viscosity.

Capturing HMA Microstructure and Permeability Results

The experiment included field cores from different Hot Mix Asphalt (HMA) pavements, laboratory specimens cored out of slabs compacted using the Linear Kneading Compactor (LKC), and open-graded Superpave gyratory compactor specimens (SGC). The HMA mixes varied in the nominal maximum aggregate size (NMAS), aggregate type, and percent air voids.

The HMA 3-D microstructure was captured using an X-ray computed tomography (CT) system. Horizontal slices of 1.0 mm thickness with an overlap of 0.2 mm were captured. These slices were stacked together in the computer to form the actual 3-D porous microstructure. An image resolution was about 0.15 mm/pixel. Images were captured in a gray scale that consists of 256 levels of gray color intensity. Each level corresponds to a different density within the asphalt mix microstructure. Figure 1a shows an example of an X-ray CT image with 1024×1024 pixels from a specimen with a diameter of 150 mm. The gray scale images were transformed to binary images of white and black phases that correspond to the solids and air voids (Figure 1b), respectively. Examples of the 3-D microstructures that are assembled from the 2-D CT scanned images are shown in Figure 2.

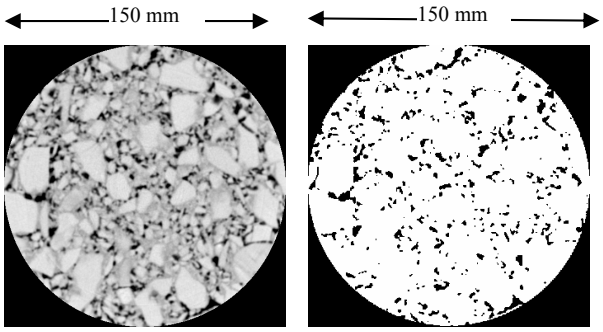

Figure 1. An example of X-ray CT image for an asphalt concrete specimen with a diameter of 150 mm. (a) Gray scale image, (b) Binary image.

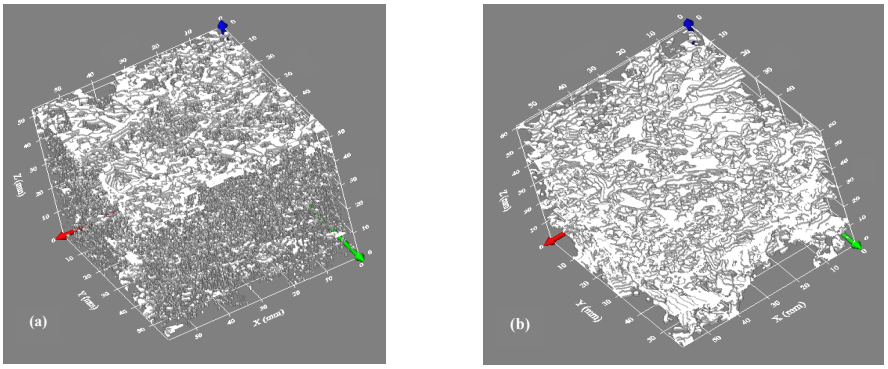

Figure 2. An example of two assembled 3-D microstructures. (a) LKC specimen with 5.5% air voids, and (b) LKC specimen with 17.4% air voids.

The numerical results for the Field, LKC, and SGC specimens are compared to the permeability calculated using the Kozeny-Carman equation (Equation 7), and using the upper limit presented by Berryman and Blair (Equation 8) [6].

$$K = \frac{C\varepsilon^3 D_s^2}{(1-\varepsilon)^2} \tag{7}$$

$$K \le \frac{4}{81}\frac{\varepsilon^3 D_s^{\ 2}}{(1-\varepsilon)^2} \tag{8}$$

where ε is the porosity, C is a constant that equals to (1/180) for spheres, and D_s is the average particle diameter. The average particle diameters (D_s) for the different mixes are calculated from gradations. A maximum value of particle diameter of 8.70 mm, and a minimum value of 2.70 mm are calculated from the different mixes. Figure 3 shows comparisons of the numerical results to the Kozeny-Carman equation, and Berryman-Blair equation. Most of the numerical results are within the two limits of the Kozeny-Carman equation, while they are less than or equal to the upper limits by Berryman-Blair equation.

The effect of porosity (or percent of air voids %AV) on HMA permeability is shown in Figure 4. It can be seen that the SGC mixes have higher permeability than the Field and LKC mixes at the same %AV. This can be attributed to the fact that the SGC open graded mixes have air voids that are more open and connected. The numerical analysis of the fluid flow in all mixes predicted the general trend of high permeability at higher %AV. This is clearly seen in the results of the SGC specimens and Field cores. On the other hand, this trend is less evident in the LKC specimens. The Field, SGC, and LKC specimens had different air void distributions due to the differences in compaction

methods [6]. These differences can lead to different permeability values at the same %AV. An example of the fluid flow simulation in a vertical section of HMA specimen is shown in Figure (5).

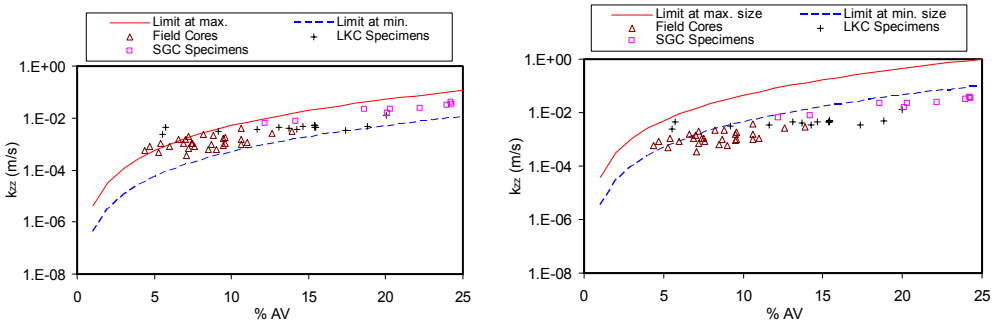

(a) Kozeny-Carman equation. (b) Berryman-Blair equation.

Figure 3: Comparisons between Numerical Predictions of Permeability and the Closed Form Solutions.

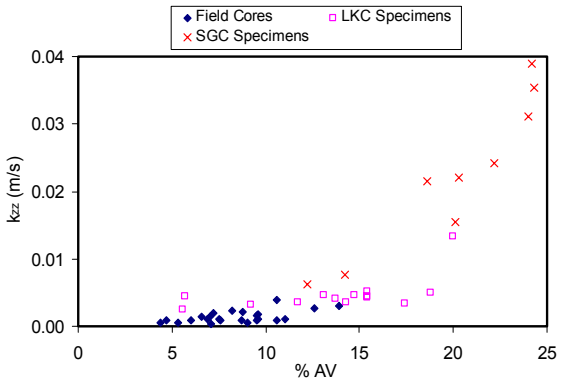

Figure 4. Permeability of asphalt mix specimens at different percent air voids (%AV).

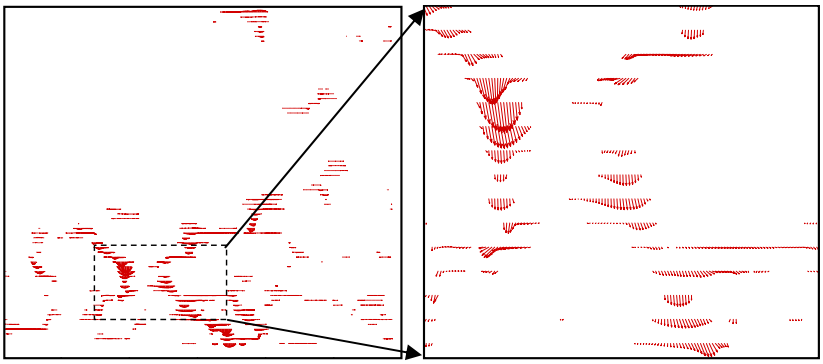

Figure 5. Velocity distribution for a vertical section in an asphalt mix specimen.

Conclusions

In this study, a numerical scheme is developed to simulate fluid flow in 3-D microstructures and to calculate permeability. The numerical model is used to simulate fluid flow in real porous media microstructures including field HMA cores, laboratory linear kneading compactor specimens, and laboratory Superpave gyratory compactor specimens. The porous media microstructures were captured using an X-ray CT system. The numerical results of permeability are compared to closed form solutions. The permeability of these materials is found to be within the upper and lower limits of the closed form solutions. However, the results emphasize that there is no unique relationship between permeability and percent air voids.

Acknowledgements

The authors acknowledge the National Science Foundation funding through grants CMS-0116793 and CMS-0134519.

Reference

1. Adler, P. M., Jacquin, C. G., Quiblier J. A. (1990). "Flow in Simulated Porous Media." *Int. J. Multiphase Flow*, Vol. 16, No. 691-712.
2. Martys, N. S., Torquato, S., Bentz, D. P. (1994). "Universal Scaling of Fluid Permeability for Sphere Packings." *Phys Rev E*, Vol. 50, pp. 403-408.
3. Masad, E., Muhunthan, B., Martys, N. (2000). "Simulation of Fluid Flow and Permeability in Cohesionless Soils." *Water Resour Res*, Vo. 36, pp. 851-864.
4. Tashman, L., Masad, E., Crowe, C., Muhunthan, B. (2003). "Simulation of Fluid Flow in Granular Microstructure using a Non-Staggered Grid Scheme." *Computers & Fluids,* Vol. 32, pp. 1299-1323.

5. Al-Omari, A., Masad, E. (2004). "Three Dimensional Simulation of Fluid Flow in X-ray CT Images of Porous Media," *International Journal for Numerical and Analytical Methods in Geomechanics. (in review)*.
6. Berryman, J. G., and Blair, S. C. (1986). "Use of digital image analysis to estimate fluid permeability of porous materials: Application of two-point correlation functions." *Journal of Applied Physics,* Vol. 60, No. 6, pp. 1930-1938.
7. Al-Omari A., Tashman, L., Masad, E., Cooley, A. Harman, T. (2002). "Proposed Methodology for Predicting HMA Permeability." *Journal of the Association of the Asphalt Paving Technologists*, Vol. 71, pp. 30-58.